

INTERPRETATION OF PULLOUT AND DIRECT SLIDING TESTS ON DOUBLE TWISTED STEEL WIRE MESH REINFORCEMENTS

V. N. Ghionna

University of Reggio Calabria, Italy

M. Olivetta

Civil Engineer– Vercelli, Italy

M. Vicari

Officine Maccaferri – Bologna, Italy

ABSTRACT: The paper deals with the numerical modelling of direct sliding and pullout tests carried out on a double twisted hexagonal steel wire mesh reinforcement confined in a uniform medium silica sand. Numerical analysis were conducted through a two dimensional finite difference code (FLAC-2D) in which a non linear elastic soil model with allowance for dilatancy and post peak softening has been implemented. The reinforcement was modelled as a linear elastic “cable element” yielding only in tension, while an elastic perfectly plastic relationship was used to model soil to reinforcement interface “equivalent” frictional behaviour. The relevant parameters (“interaction coefficients”) were determined by back analysis of pullout tests results at best-fit of the axial load vs. displacement curves. Back-figured values of shear strength interaction coefficients (α_b) in pullout tests resulted half of the corresponding ones experimentally determined in direct sliding tests, while stiffness interaction coefficients (K_b) in pullout tests resulted approximately equal to those experimentally determined in direct sliding tests.

1 INTRODUCTION

Load-displacement curves from pullout tests (PO) on extensible reinforcements reflect the integrated behaviour of the overall length of the reinforcing unit.

Tensile stress and strain patterns along the reinforcements are not uniform and tend to decrease from the pulling extremity to the opposite one.

This makes difficult to extrapolate the results obtained from one test to others (i.e. different overburden stresses, reinforcement lengths, etc.) unless a reliable model of the “local” load transfer mechanism from the reinforcement to soil is adopted. This model can be considered a constitutive relationship of the interface behaviour.

For continuous reinforcements (such as geotextiles and geomembranes) the basic load transfer mechanism is purely frictional and it can be deduced from the behaviour observed in interface direct sliding (DS) tests.

However for mesh type reinforcements (such as geogrids, double or triple twisted steel wire mesh nets, etc.) interaction mechanism is governed not only by the frictional soil to soil and soil to solid surfaces phenomena but also by the passive resistance mobilised in the front soil by the transverse members (Jewell, 1996).

For such reinforcements an “equivalent” interface frictional model can still be defined (Jewell, 1996) but the relevant stress-strain parameters (“bonding parameters”) can’t be deduced from the results of direct sliding tests. Jewell (1996) proposed analytical expressions for the equivalent ultimate sliding resistance (“bond capacity”) of these reinforcements.

However these expressions are valid for rectangular rigid meshes and their extrapolation to more complex geometries and deformation patterns (such as those characterising the hexagonal double-twisted steel wire meshes considered in this study) is questionable.

Analytical solutions for predicting pullout tests results on geotextiles using an approach similar to that proposed by Frank and Zhao (1982) for soil nails have been reported by several authors using different shear stress vs. relative displacement “local” frictional law such as a linear elastic-

perfectly plastic one (Bollo-Kamara et al., 1995) or a hyperbolic one (Gurung, 2000).

Bollo-Kamara et al. (1995) presented a comparison between the basic parameters of the linear elastic-perfectly plastic law (namely ultimate frictional shear stress τ_b and interface stiffness coefficient k_b defined in fig. 7) back-figured from pullout tests and direct sliding tests carried out on the same materials.

Back-analyses of experimental data were carried out using an analytical procedure based on Frank and Zhao (1982) approach. Basing on previous results of Alfaro et al. (1995), Gurung (2000) suggested to derive the “local” equivalent friction law for geogrids from pullout tests carried out on short geogrid specimens (“element tests”), but the reliability of this approach needs to be more carefully investigated.

Lo (1990) conducted “embedded” tension tests in sand on a double twisted steel wire mesh reinforcement (similar to that adopted in the present research) in a large split-box with the aim to ascertain possible changes in breaking load and linear axial stiffness due to the confined conditions.

More recently in FEM analyses with PLAXIS code, Bergamo et al. (2000) proposed to model the interaction behaviour of a hexagonal steel wire mesh reinforcement through “thin layer” elements characterised by a linear elastic-perfectly plastic law. The relevant parameters (namely: interface friction angle δ_i , cohesion c_i , and shear modulus G_i) were generated from the corresponding ones of the soil (ϕ' , c' and G) by using an interaction coefficient (R) as follows:

$$\tan \delta_i = R \tan \phi'$$

$$c_i = R c'$$

$$G_i = R^2 G$$

R values were determined by back-analyses of pullout tests and direct sliding tests results conducted through PLAXIS code. For the two types of hexagonal steel wire mesh reinforcements considered in the study (namely: a

zinc coated one and a PVC coated one) embedded in silty sand, the following values of R were obtained:

R = 0.3 to 0.5 in pullout tests

R = 0.9 in direct sliding tests

The value R=0.9 back-figured from direct sliding tests was consistent with the theoretical interaction coefficient (α_{ds}) evaluated through Jewell (1996) expression.

Bergado and Voottipruex (2000) proposed also an analytical method to derive the complete "local" equivalent interface shear stress vs. relative displacement curve from pullout test results without making any a-priori assumption about the model adopted.

As a further development Bergado et al. (2001) proposed an analytical method to derive the pullout load vs. elongation curve of hexagonal steel wire mesh reinforcements embedded in granular soil by taking into account separately all patterns of the deformational behaviour of the hexagonal cells, namely: translation in the pull direction and deformation of the cell shape ("necking"). The method assumes a hyperbolic stress-strain function to model the bearing resistance of the transverse members and a linear elastic-perfectly plastic relationship for the friction resistance.

The research described in the present paper aims at providing a contribution to the modelling of the interface behaviour of a double-twisted steel wire mesh reinforcement in contact with sand in both direct sliding and pullout tests. An experimental test program was conducted in a large split box capable of allowing interface direct shear tests and pullout tests to be carried out with the same basic apparatus by simply substituting the upper half box.

A linear elastic-perfectly-plastic "local" equivalent shear stress vs. relative displacement interfacial law was assumed for both direct shear and pullout tests interpretation.

Model parameters for pullout tests were back calculated from pullout test results by numerical analyses conducted through a two-dimensional finite difference code (FLAC-2D). Finally local bonding coefficient (α_b) and stiffness coefficient (K_b) back-figured from pullout tests were compared with the corresponding ones determined in direct sliding tests.

2 LARGE DIRECT SHEAR BOX

The modified direct shear box adopted in this research was specifically designed to perform strain controlled direct sliding tests on samples of large dimensions (fig. 1)

This allows mesh type reinforcement panels with an adequate number of meshes in both longitudinal and transverse directions to be investigated.

The box consists of two overlapped steel halves, the upper one being fixed while the lower moves horizontally through a roll-bearing equipped sliding block.

The upper half-box has internal dimensions, 0.7 m by 0.7 m and houses the fill soil while the lower half-box has dimensions 0.7 m by 1.5 m and is filled with a low density concrete block levelled on the surface in order to obtain a rigid platform that supports a steel plate on which the wire mesh panel is welded.

To simulate (as in the real cases) the presence of the soil on both side of the reinforcing panel, a thin layer of sand is glued on the supporting steel plate. A lubricant system constituted by a thin film of grease coated with a protective polyethylene sheet is applied on the internal walls of the upper half-box to reduce friction on the soil.

Vertical loads are applied through a rigid steel top plate actuated by a hydraulic piston, while horizontal forces are provided by a load actuator acting on the lower half-box.

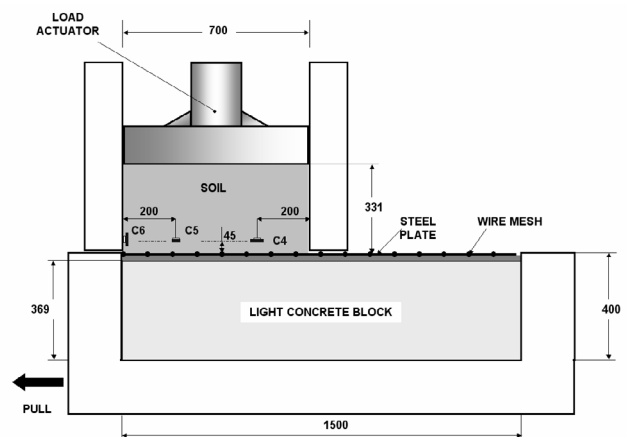


Figure 1 Cross-section of the direct shear test apparatus

For both vertical and horizontal directions a load cell is used for measuring the forces, while vertical and horizontal displacements are measured by LVDT's. In the tests carried out the rate of displacement of the lower half-box was set equal to 0.7 mm/min. Soil samples were reconstituted in layers compacted through the tamping method up to reaching the prefixed relative density (D_R).

Horizontal total pressure cells (C) are installed at a small distance above the reinforcement to verify the uniformity of the vertical pressures distribution on the sliding plane during the sliding phase.

3 LARGE PULLOUT APPARATUS

Pullout apparatus consists of two superimposed half-boxes having plane internal dimensions of 1.5 m by 0.7 m (fig. 2).

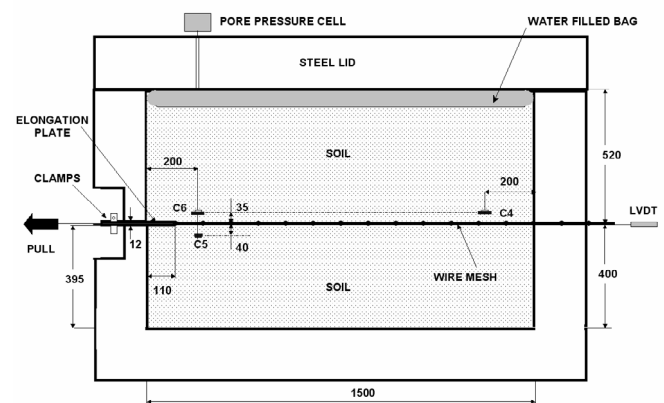


Figure 2 Cross-section of the pullout test apparatus

The fill material is placed inside the box in layers compacted through the tamping method up to the same relative density adopted in DS tests. Once the filling operation is completed, the box is closed by a rigid steel lid. On the lower side of the lid is mounted a water filled cushion that allows to apply uniform vertical pressures on top of the sample.

Reinforcement panels are pulled out from the front wall and are free to translate at the rear extremity. Two thin slots 12 mm in thickness are machined respectively one on the front wall and the other on the rear wall of the box, to allow panel extensions to cross them.

Pullout forces are applied to the panels through smooth elongation steel plate 8 mm in thickness penetrating into the fill material for a distance of 110 mm. This prevents

that during the pulling phase some portion of the reinforcement panel be pulled out in air.

Preliminary calibration tests, under different vertical pressures have been conducted on the elongation plate immersed in soil in order to correct the measured force for the effects caused by its presence. Vertical pressures are applied by pressurising the water cushion. A pore pressure transducer is used to monitor them.

Pullout tests are carried out under strain-controlled condition using the same horizontal load actuator adopted in direct shear tests. In the present research tests were run at a constant strain rate of 0.7 mm/min. A load cell is adopted to measure pullout forces while front and rear horizontal displacements of the panels are monitored by means of LVDT's.

Horizontal total pressure cells (C) have been installed in the fill material to check the uniformity of the vertical pressures acting on the panel during both the uniaxial consolidation phase and the pulling phase. Furthermore in one test external LVDT's connected by metallic wires to discrete points of the panel have been used to measure the trend of the axial displacement along the panel during pull-out tests. For space limitations these data have not been presented in the present paper.

4 MATERIALS ADOPTED

4.1 Reinforcement

The reinforcement panels adopted consist of double-twisted hexagonal steel wire mesh provided with a PVC protective coating (Green Terramesh) manufactured by Oficine Maccaferri.

The geometrical features of the reinforcement meshes are shown in fig. 3.

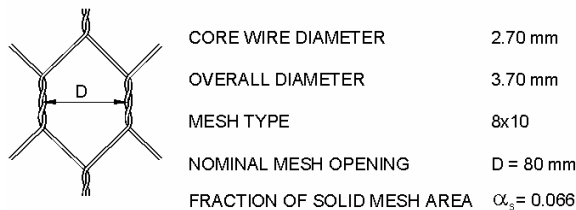


Figure 3 Characteristics of the double twisted steel wire mesh reinforcement

Tensile strength in air ("nominal breaking load", NBL) when tested in accordance with ASTM A 975-97 and linear deformation modulus (J) at failure strain were as follows:

$$\text{NBL} = 50.4 \text{ kN/m}; \text{ J} \approx 500 \text{ kN/m}$$

4.2 Soil

Soil adopted as fill material was a medium uniformly graded natural silica sand (Ticino sand) that has been in the past extensively investigated from the geotechnical point of view.

Strength and deformability parameters obtained from triaxial and resonant column tests carried out on specimens reconstituted at the same relative density ($D_R = 80\%$) as that considered in the present research are summarised below:

- peak friction angle $\phi'_p = 43^\circ$
- drained cohesion $c' = 0$
- constant volume friction angle $\phi'_{cv} = 34^\circ$

- small strain shear modulus $G_o = 630$ to 900 kPa (for σ_c ranging from 25 to 50 kPa)

Beside the aforementioned tests the sand was subjected to direct shear tests in the large direct shear box described in par. 2.

These tests were aimed at providing a common experimental basis for the determination of the direct sliding interaction coefficient (α_{ds}) from both soil to reinforcement and soil to soil direct shear tests. This approach was also followed by other researchers (e.g. Bergado and Vootti-pruex, 2000)

5 TEST PROGRAM AND RESULTS

5.1 Direct sliding tests

Three different interface direct shear tests were carried out at effective vertical pressures (σ'_v) ranging from 50 kPa to 200 kPa.

The ultimate peak and residual (large displacement) shear force (respectively T_{ult}^p and T_{ult}^r) along with the corresponding direct sliding shear strength interaction coefficients (α_{ds}^p and α_{ds}^r) obtained in each test are listed in table 1.

Table 1 Direct sliding tests results

Test	σ'_v (kPa)	τ_{ult}^p (kPa)	τ_{ult}^r (kPa)	U_{50} (mm)	U_p (mm)	α_{ds}^p	α_{ds}^r	K_{ds}^{50} (kPa/mm)	K_{ds}^p (kPa/mm)
T1	100	116	88	1.96	6.9	1.01	0.98	29.6	26.7
T2	200	220	174	2.80	11.5	0.96	0.97	39.3	28.5
T3	50	62	47	1.96	6.9	1.06	1.04	15.6	14.2

Values of α_{ds} were evaluated from the following expressions:

$$T_{ULT}^p = \sigma'_v \cdot \alpha_{ds}^p \cdot \tan\phi'_p \cdot L \cdot B$$

$$T_{ULT}^r = \sigma'_v \cdot \alpha_{ds}^r \cdot \tan\phi'_{res} \cdot L \cdot B$$

by assuming for ϕ'_p and ϕ'_{res} respectively the peak and residual friction angles obtained in the soil to soil direct shear tests mentioned in par. 4.2.

In the previous expressions L and B represent, respectively, the length and the width of the panels adopted in the tests (L = B = 0.7 m).

Fig. 4 reports the shear force vs. displacement curves obtained in the direct sliding tests.

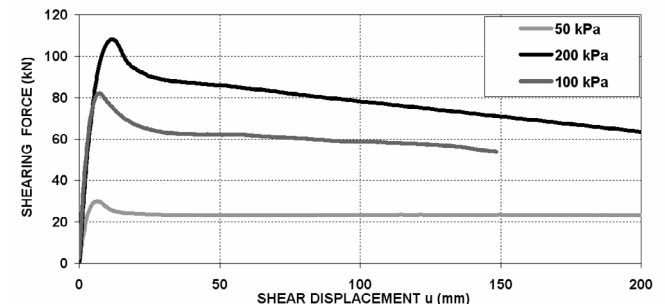


Figure 4 Direct sliding tests results

The aforementioned values of α_{ds} are in good agreement with the theoretical ones determined from the expression (Jewell, 1996):

$$\alpha_{ds} = \alpha_s \frac{\tan \delta}{\tan \varphi'} + (1 - \alpha_s)$$

Using: $\alpha_s = 0.066$ (see fig. 3) and $\tan \delta \cong 0.6 \cdot \tan \varphi'$ (smooth solid surface), such expression gives for both peak and residual conditions the following average values:

$$\alpha_{ds}^p \approx \alpha_{ds}^r \approx 0.97$$

In table 1 are also reported the interface stiffness interaction coefficients (K_{ds}^p and K_{ds}^{50}) determined after linearisation of the shear stress (τ) vs. horizontal displacement (u) direct sliding curves according to the two linearisation criteria evidenced in fig. 5.

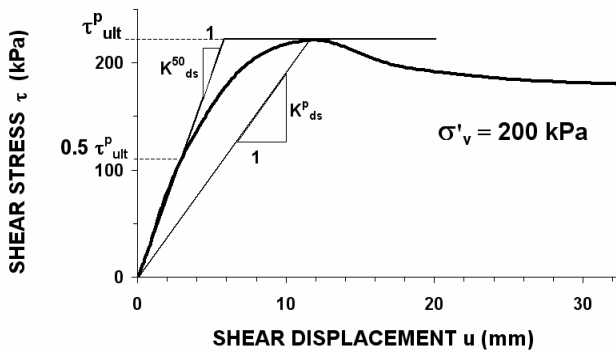


Figure 5 Determination of K_{ds} from interface direct shear tests

The following expressions were used for their evaluation:

$$K_{ds}^p = \frac{\tau_{ULT}^p}{u_p}; \quad K_{ds}^{50} = \frac{0.5 \cdot \tau_{ULT}^p}{u_{50}}$$

being: u_p, u_{50} = respectively, horizontal displacements at $\tau = \tau_{ULT}^p$ and $\tau = 0.5 \cdot \tau_{ULT}^p$. Results obtained evidenced a dependence of K_{ds} on σ'_v . In the lower range of σ'_v ($\sigma'_v < 100$ kPa) this dependence seems to be linear and corresponding to the following relationships:

$$K_{ds}^{50} = 0.3 \sigma'_v \text{ (kPa/mm)}$$

$$K_{ds}^p = 0.17 \sigma'_v \text{ (kPa/mm)}$$

with σ'_v expressed in kPa.

5.2 Pullout tests

Two pullout tests were carried out at σ'_v values reported in tab. 2

Table 2 Pullout tests results

Test	σ'_v (kPa)	F_{max}/W (kN/m)	ΔL_{max} (mm)	α_{po} (adim)	J_{po}^f (kN/m)	$J_{po}^{0.5}$ (kN/m)	J_{po}^1 (kN/m)
PO2	50	49.8	35	-	1945	4862	2258
PO3	25	40.6	45	0.50	1259	4045	1850

However only test PO3 reached a complete sliding condition. In test PO2 mesh breakage occurred before any rear displacement was observed. Fig. 6 shows the tensile force per unit width (F/W) vs. the elongation ($\Delta L/L$) curves observed in the two tests.

The maximum tensile force per unit width of the reinforcement (F_{max}/W) measured in the tests along with the

corresponding elongation at the pulled extremity (ΔL_{max}) determined as difference between front and rear displacements are reported in tab. 2

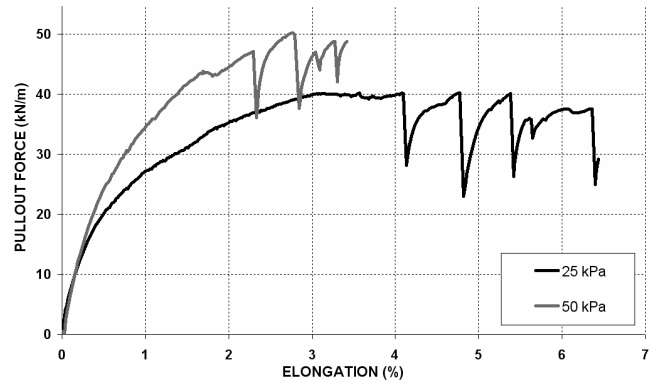


Figure 6 Pullout test results at $\sigma'_v = 25$ and 50 kPa

In the same table are also shown the values of the “global” pullout interaction coefficient (α_{po}) and the “global” linear axial stiffness in confined conditions (J_{po}^f and $J_{po}^{0.5}$) measured in the tests. Values of α_{po} in tab. 2 were determined from the following expression:

$$F_{max} = 2 \sigma'_v \cdot \alpha_{po} \cdot \tan \varphi' \cdot L \cdot B$$

assuming for φ' the same value adopted for the interpretation of direct sliding tests (see point 6.2) and for L and B (panel dimensions) the following values:

$$L = 1.395 \text{ m}; \quad B = 0.682 \text{ m.}$$

The confined moduli J_{po}^f and $J_{po}^{0.5}$ were evaluated after linearisation of the pulling force per unit width vs. the elongation curve using the same linearisation criteria adopted for the direct shear tests (fig. 5).

6 NUMERICAL MODELLING OF PULLOUT TESTS

Numerical modelling of pullout tests was carried out by means of a two-dimensional finite difference code (FLAC-2D). A sub-routine was added to the commercial version of the code in order to implement a new non-linear constitutive law for granular soils. The numerical model adopted consists of the following three elements:

- soil
- reinforcement
- interface between soil and reinforcement.

The relevant constitutive relationships are described in the following paragraphs. Preliminarily it has been considered useful to report some brief remarks on the criteria adopted for their choice.

6.1 Models adopted

6.1.1 General remarks

The researches carried out in the last 15 years about the frictional behaviour of a solid surface in contact with a granular soil (Boulon, 1989; Porcino et al., 2003) have shown that it depends on a very thin soil layer (called “interface”) whose thickness is approximately 5 to 10 times the average grain size (D_{50}) of the soil.

This is a zone where very high shear deformations occur, while the adjacent soil remains relatively uninvolved acting predominantly as an “elastic” restraining medium against the dilative or compressive volumetric changes of the interface (Boulon, 1989).

The aforementioned considerations justify the following considerations:

a) the interface behaves like an independent material obeying a stress-strain relationship completely different from that of the adjacent soil; the capability of the model to correctly account for dilatancy effects is important;

b) interfacial dilatancy effects are enhanced by three-dimensional geometrical features of the reinforcement (i.e. mesh or strip type reinforcements). On the opposite they are relatively unimportant in continuous reinforcements, subjected to uniform vertical pressures;

c) the restraining effects of the adjacent soil are mainly controlled by its stiffness in a moderate range of shear strains. This enhances the need of an accurate modelling of soil deformability. Since stress-strain relationships of granular soils are highly non-linear even at relatively small strains, a non-linear soil model should be more appropriate;

d) a theoretical model capable to capture the most important aspects of the dilatancy behaviour of an interface between solid surfaces and granular soils has been recently proposed by Ghionna and Mortara (2002). However it is very complex and not yet particularised for mesh type reinforcements. Other simplified models, such as those available in commercial codes, are not sufficiently reliable for the parameters easily linkable to traditional tests results.

For this reason in the present study it has been preferred to use a non-dilatative interface model coupled with a soil model in which a non associated flow rule based on the maximum value of the dilatancy angle (Ψ) is adopted.

6.1.2 Soil

Soil model adopted for Ticino sand is a non-linear elastic model associated to a curved Mohr-Coulomb failure criterion with allowance for dilatancy, and post-peak softening.

Non linear stress-strain behaviour is taken into account by means of a shear modulus degradation law of the hyperbolic type proposed by Lee and Salgado (1999).

This law expresses the ratio (G/G_0) between the secant and the initial shear modulus in terms of the first (I_1) and second (J_2) stress invariant and assumes for the initial shear modulus G_0 a dependence from the effective mean normal stress (σ'_m) according to Hardin and Black (1966) relationship. A constant value of the dilatancy angle (Ψ) is assumed and it corresponds to the maximum value provided by Bolton's (1986) theory. Post-peak softening is modelled through an expression linking the post-peak mobilised friction angle (ϕ'_m) with the current plastic shear strain (γ^p). This relationship is empirically determined from triaxial tests results.

6.1.3 Reinforcement

The double-twisted steel wire mesh reinforcement was modelled through a linear elastic one-dimensional axial element ("cable element") with no flexural rigidity and yielding only in tension characterised by the following parameters:

- tensile strength $T_{ult} = 50$ kN/m
- "elastic" elongation modulus $J = 500$ kN/m

The adopted value of J was coincident with that determined from the tensile tests in air reported in par. 4.1. However, in spite of the fact that such tests were conducted with a procedure specifically designed to account in some way for the restraining effects induced by soil grains entrapped into the meshes, it is to be expected that the obtained values could not be fully representative of the real behaviour in confined conditions.

For this reason, after a first phase in which FLAC analyses were carried out with the experimental value of J

specified above, a parametric study was also conducted in order to ascertain whether this value is still reliable for confined conditions.

In such parametric study J was varied in a range from 500 kN/m to 5000 kN/m.

6.1.4 Interface

Interface has been modelled through "grout" elements represented by "spring-slider" systems located at the nodal points (fig. 8).

The shear behaviour of the "grout" elements during the relative displacement between reinforcement and soil is described numerically by a linear elastic perfectly-plastic relationship (fig. 7) characterised by the following parameters:

- K_b = interaction ("bonding") stiffness coefficient
- τ_b = ultimate ("bonding") shear strength.

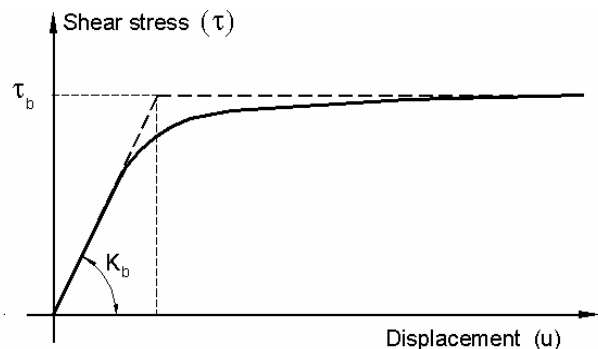


Figure 7 Shear behaviour of the grout elements

Furthermore a purely frictional model (i.e. zero cohesion) has been assumed for τ_b according to the following expression:

$$\tau_b = \sigma'_v \cdot \alpha_b \cdot \tan \phi'_p$$

where α_b = interaction ("bonding") strength coefficient. Values of α_b and K_b were evaluated from back-analysis of pullout tests at best fit of the load-displacement curves obtained in such tests.

6.2 FLAC analyses

A 4 nodes equilateral grid, 920 mm in height and 1500 mm in length, was adopted in FLAC calculations (fig. 8).

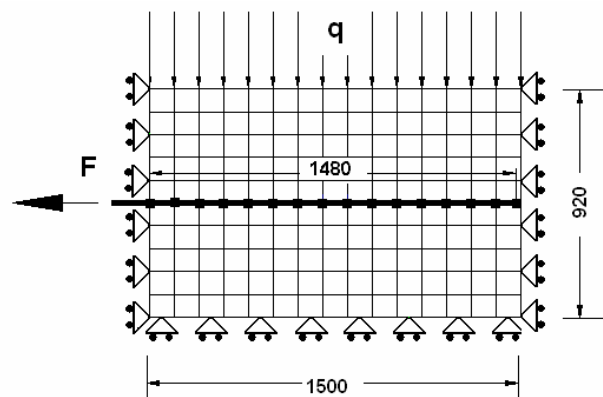


Figure 8 FLAC pullout test modelling

Side and bottom walls were considered to be rigid and perfectly smooth. A uniform vertical pressure (q) was ap-

plied on top of the soil. Calculations were carried by applying to the pulling extremity of the cable element subsequent loading steps and evaluating the relevant elongations. Evaluation of pullout curve was repeated for several combinations of α_b and K_b and the values corresponding to the best fit of the experimental curves were retained. Finally a parametric analysis was conducted on J as mentioned in par. 6.1.3.

7 NUMERICAL ANALYSIS RESULTS AND CONCLUSIONS

Figs. 9 show the best fit predictions of the load/displacement curves obtained in tests PO2 and PO3.

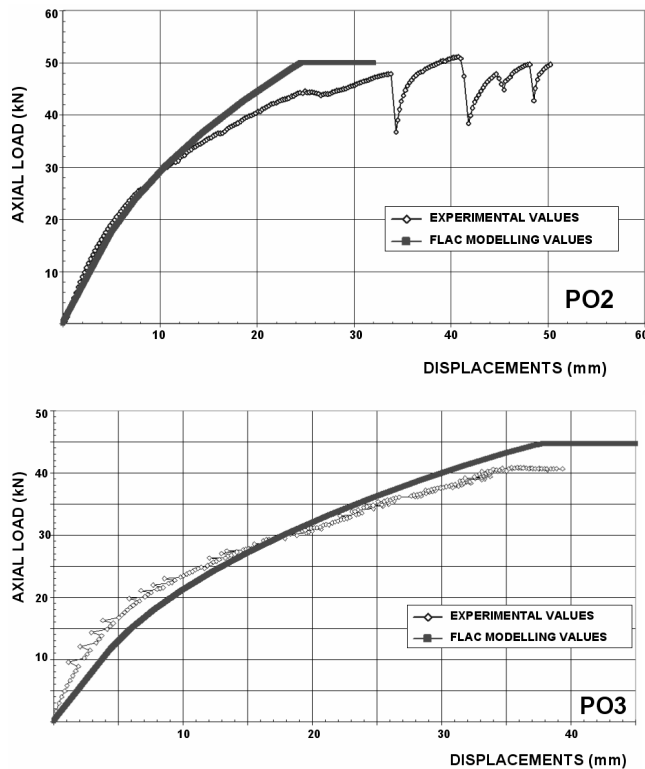


Figure 9 Experimental vs. predicted pullout test results.

Such predictions were based on the following parameters:

- Test PO2
 - $\alpha_b = 1$
 - $K_b = 9.8 \text{ kPa/mm}$
 - $J_b = 500 \text{ kN/m}$
- Test PO3
 - $\alpha_b = 1$
 - $K_b \cong 4.9 \text{ kPa/mm}$
 - $J_b = 500 \text{ kN/m}$

Comparing these values with data reported in Tab. 1 the following conclusions can be drawn:

- a) the interaction strength coefficient (α_b) is approximately half of α_{ds}
- b) the interaction stiffness coefficient K_b is practically coincident with K_{ds}^p
- c) the elongation modulus of the double twisted wire mesh panel in immersed condition is equal to the nominal value J determined in air.

Such conclusions confirm the existence of a different interaction mechanism between pullout and direct shear tests with values of interaction strength coefficient (α_b) in pullout tests being significantly smaller (50%) than those determined in direct shear tests.

However such different mechanism doesn't seem to have an impact on interaction stiffness coefficients (K_b).

Furthermore, the procedure adopted for testing hexagonal steel wire mesh reinforcements in air seems to be adequate for reproducing their deformational behaviour in confined conditions.

8 REFERENCES

- Alfaro M.C., et al., 1995: *Soil-geogrid reinforcement interaction by pullout and direct shear tests*. Geotechnical Testing Journal Vol. 18, N° 2.
- Bergado D.T., Teerawahanasuk C., Yonwal S. and Voottipruex P., 2000: *Finite element modelling of hexagonal wire reinforced embankment on soft clay*. Canadian Geotechnical Journal Vol. 37, pp. 1209-1226.
- Bergado D.T. and Voottipruex P., 2000: *Interaction coefficient between silty sand backfill and various types of reinforcements*. Proc. 2nd Asian Geosynthetics Conference, Kuala Lumpur, Malaysia.
- Bergado D.T., Teerawahanasuk C., Wongsawanon T. and Voottipruex P., 2001: *Interaction between hexagonal wire mesh reinforcement and silty sand backfill*. ASTM Geotechnical Testing Journal Vol. 24 N° 1, pp. 23-28.
- Bollo-Kamara N., Bordeau Y., Bahloul F. and Ozunro V., 1995: *A study of friction mobilization at a soil/geotextile interface using a bi-dimensional analogic model*. Geosynthetics '95.
- Bolton M.D., 1986: *The strength and dilatancy of sands*. Géotechnique 36 (1), pp. 65-78.
- Boulon M., 1989: *Basic feature of soil-structure interface behaviour*. Computers and Geotechnics, Vol. 9, N° 1-2, pp. 47-58.
- Frank R. and Zhao S.R., 1982: *Estimation through pressuremeter parameters of the settlement under load of drilled shafts in fine soils*. Bulletin de liaison des laboratoires des Ponts et Chaussées No. 19, Réf 2712, pp. 17-24.
- Ghionna V.N. and Mortara G., 2002: *An elastoplastic model for sand-structure interface behaviour*. Géotechnique, Vol. 52, N° 1, pp. 41-50.
- Gurung N., 2000: *A theoretical model for anchored geosynthetics in pullout tests*. Technical note. Geosynthetics Intl. Journal Vol. 7, N° 3.
- Hardin B.O. and Black W.L., 1966: *Sand stiffness under various triaxial stresses*. Journ. Of Soil Mechanics and Foundation Engineering Division ASCE, 89 (SM1), pp. 33-65.
- Jewell R.A., 1996 *Soil Reinforcement with Geotextiles*, CIRIA Special Publication 123. London CIRIA.
- Lee, J. and Salgado R., 1999: *Analysis of calibration chamber plate load tests*. Canadian Geotechnical Journal Vol. 37, pp. 15-25.
- Lo S.C.R., 1990: *Determination of design parameters of a mesh-type soil reinforcement*, ASTM Geotechnical Testing Journal, Vol. 13, N° 4.
- Porcino D., Fioravante V., Ghionna V.N., Pedroni S., 2003: *Interface Behaviour of Sands from Constant Normal Stiffness Direct Shear Tests*. Geotechnical Testing Journal Vol. 26, N° 3, pp. 289-301.